Acceleration in the Heliosphere

E. Möbius[a] and R. Kallenbach[b]

[a]*Space Science Center and Department of Physics, University of New Hampshire, Durham, USA*
[b]*International Space Science Institute, Bern, Switzerland*

Introduction

Since the discovery by Victor Hess on a balloon flight in 1912 that the intensity of energetic radiation increases with altitude, it has been known that cosmic rays are an important ingredient of the space environment. The space era has opened this important phenomenon to detailed study. The extension of optical astronomy into the radio regime in the 1940's, and later with space-based telescopes into the more energetic X-ray and γ-ray regimes, has provided ample evidence for humongous and violent objects in the Universe[1] that generate floods of extremely energetic particles, which ultimately form the cosmic-ray population in our galactic neighbourhood. Our living environment on Earth can be affected by this potentially dangerous radiation and its mutation-driving impacts, but it is very effectively protected by a three-layer shield system: (1) the heliosphere with the solar wind and its embedded magnetic field; (2) Earth's magnetic field; (3) Earth's atmosphere. Satellites and space probes have gathered information about the variation in the radiation intensity and spectra in response to changes in the interplanetary medium and solar activity[2,3]. They have also provided us with in-situ observations of sources, acceleration, and transport of energetic particles generated in our immediate neighbourhood, in and around Earth's magnetosphere, at the Sun, and throughout the heliosphere. Our ability to model and scale acceleration processes enables us to understand not only our own environment, but also that of distant particle accelerators, which cannot be studied in-situ. As shown in Figure 1, the average fluence spectra in interplanetary space[4] extend from the solar wind up to several 100 MeV/atomic mass unit [amu] with a power law for most of the range similar to cosmic rays. Shock waves, or structures where the solar wind flow is abruptly decelerated from super- to sub-sonic speeds, have been identified as powerful particle accelerators in the heliosphere. They serve as a model for supernova blast waves, which accelerate galactic cosmic rays. With ever-increasing sophistication in spacecraft instrumentation, we make good use of the laboratory on our front doorstep by simultaneously observing source and energetic-particle populations as well as magnetic and electric fields near shocks. Yet the first step from the bulk plasma into the accelerated distribution (marked with ? in Fig. 1) is still very much under debate.

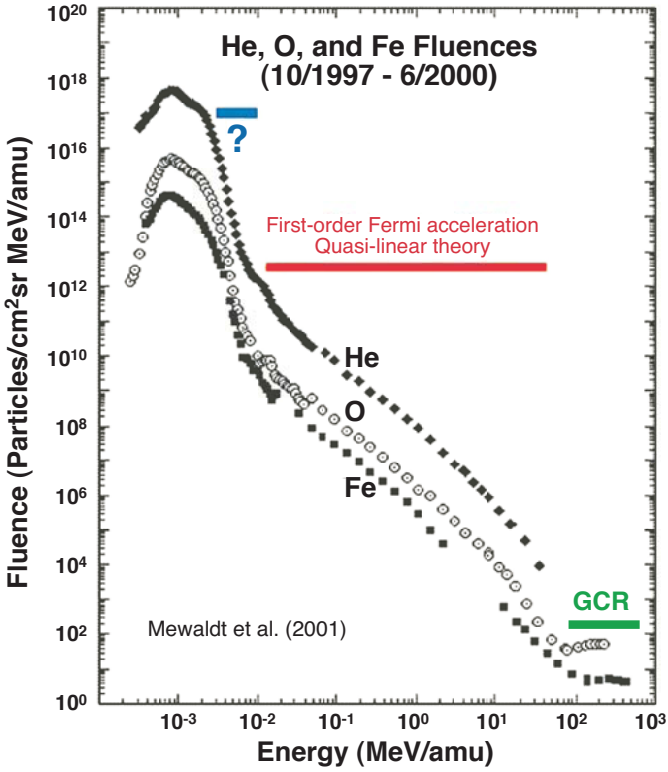

Figure 1. Total fluence spectra during the rise to the 2000 solar maximum. Solar and heliospheric energetic particles reach to galactic cosmic rays (adapted from Ref. 4).

As this brief introduction shows, particle acceleration is a genuinely interdisciplinary topic, which benefits greatly from collaborations across the dividing lines between disciplines. The International Space Science Institute (ISSI) is providing an excellent forum for such discussions with workshops and scientific teams composed of scientists with a variety of backgrounds. For cosmic rays, ISSI's impact has already been demonstrated through several cross-discipline books from such activities on the topic.

Taking a more local view, it also happens that ISSI in its first ten years of existence has hosted symposia and working teams that have compiled comprehensive summaries, provided a critical evaluation of our current understanding, and focused on the open questions for two of the key heliospheric phenomena, which are generators of energetic particles, co-rotating interaction regions (CIRs)[5] and coronal mass ejections (CMEs)[6]. CIRs are the dominant structures and generators of energetic particles in interplanetary space close to and during the solar

activity minimum. The combination of a rotating Sun and an orderly emission pattern of fast and slow solar wind leads to the periodic overtaking of slow by fast wind, with the formation of compression regions and shocks. CMEs constitute blast waves from eruptions in the solar corona and thus are dominant during solar maximum. Both types of shocks, those of CIRs and of CMEs, in fact also serve as model cases for the heliospheric termination shock, the structure at presumably about 100 astronomical units (AU) where the solar wind undergoes its final transition from supersonic to subsonic flow. The study of the heliospheric termination shock has become an ISSI research area specially funded by INTAS in Brussels, supporting the collaboration between theoreticians of the countries belonging to the former Soviet Union and scientists from the European Union or Switzerland.

The basic ISSI consensus on particle acceleration in the heliosphere formulated in the CIR book is that: (1) both solar wind and interstellar gas penetrating the heliosphere contribute as important sources to the energetic particles; (2) shocks themselves provide a means for efficient acceleration; and (3) particles are required to attain a minimum energy to be injected into shock acceleration, termed the "injection threshold", which is substantially higher than the thermal energy of solar wind particles, and may at times be higher than the maximum energy of pickup ions from neutral gas. We have organized this paper such that we devote a section to each of these three issues following this introduction, ending with the injection problem, i.e. the question of how particles make the transition from being a member of the bulk source to entering the energetic-particle population. This has been thoroughly debated in the CIR book, but basically left unsolved. We will close with a brief summary of where we stand right now, what the open issues are, and how we can apply the local results to more distant phenomena in the Universe.

Locations and Sources for Particle Acceleration

Let us start with the question of how we can identify where particles are actually accelerated. In the following we will repeatedly refer to Figure 2, which shows a simplified view of the heliosphere with rather schematic shapes for a CME and a CIR. The figure also contains the simplified spatial distribution of the most important source populations for particle acceleration, as they have been identified observationally.

Particle acceleration, where?

In the 1960's so-called "energetic storm particles" (ESP) were observed in interplanetary space with maximum intensity when the disturbance passed the space-

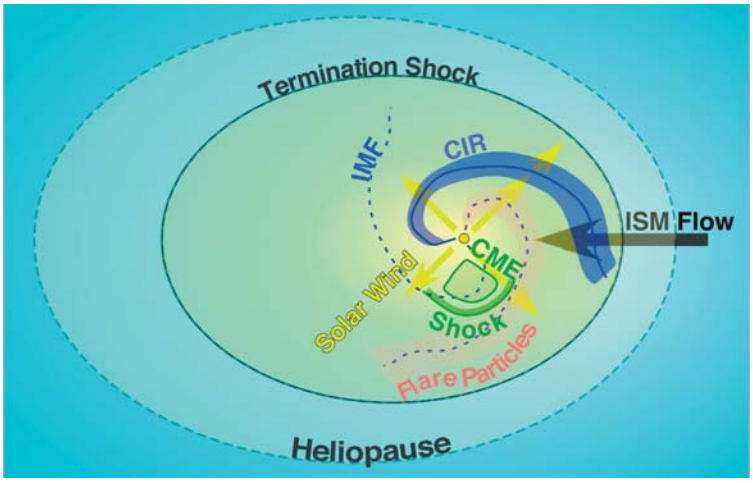

Figure 2. Schematic view of the heliosphere with interstellar medium (ISM) flow, solar wind and interplanetary magnetic field (IMF). Acceleration structures, such as a co-rotating interaction region (CIR) and a coronal mass ejection (CME), are also sketched.

craft after a major eruption on the Sun. The peak of the particle flux could be associated with the passage of interplanetary shocks that signal the arrival of a CME (shown in green in Fig. 2), and the co-location therefore suggested a causal connection with local acceleration.

Spacecraft also detected energetic particles that appeared to be connected with recurrent activity regions on the Sun. Pioneer 10 and 11 found that the fluxes increased with distance from the Sun, rather than decreasing, as is expected for a solar origin[7]. They peaked at 3-4 AU and then declined sharply. Evidence for local acceleration of these particles was the close association of the peak fluxes with the leading and trailing edge of the compression ahead of high-speed solar-wind streams[8], indicated in blue in Figure 2. CIRs are the dominant structures in the inner heliosphere during the decline and minimum of the 11-year solar cycle when the solar magnetic field is a fairly stable dipole, which is tilted relative to the Earth's orbit. Let us use a lawn sprinkler as an analogy: While the sprinkler ejects water, the rotating Sun emits solar wind. It emits fast wind from the strongly tilted northern and southern caps, and slow wind from the equator. Over the course of one rotation, a succession of slow and fast wind is seen in the ecliptic. As a consequence, the fast wind runs into slow wind that was emitted earlier, and compression regions form at the interface, the CIRs. Since even the speed difference is supersonic, shocks form on both sides of the compressions as the "sprinkler" spiral is wound up at larger distances.

Source populations for acceleration

For CMEs and CIRs, acceleration occurs in regions where plasmas with different speed converge. But what is the material that is accelerated? Composition measurements can identify the source populations. With the accelerating structures, Figure 2 also shows typical spatial distributions of major particle sources in the heliosphere. Streaming away from the Sun, the corona and solar wind are key plasma sources, with an elemental composition similar to the Sun and highly ionized because of the high temperature. Comprehensive surveys of solar energetic particles have established that the average composition of strong particle events, which are associated with CMEs, closely resembles that of the corona and solar wind[9]. These observations led to the paradigm that this energetic particle population is mostly accelerated out of the corona and/or the solar wind. The energetic ion composition in CIRs was also found to be similar to that of solar energetic particles and solar wind, but with some noticeable differences[8], in particular for He and C.

The advent of high resolution and collection power composition instruments for both bulk distributions and energetic-particle populations on spacecraft, such as ACE, SAMPEX, SOHO, Ulysses and Wind, has made it possible to establish the composition patterns, energy spectra, and spatial and temporal variations of sources and energetic particles in detail. Substantial deviations from the previously obtained averages and huge variations, which were mostly hidden in the past because of lack in resolution and counting statistics, have now called for additional energetic-particle sources. Substantial ^{3}He enhancements were found in CME events[10], which cannot be explained by selective acceleration out of the solar wind, as its ^{3}He abundance is very low[11]. However, ^{3}He and heavy ion enrichment have long been known as the hallmark of impulsive flares[12]. In fact, the active Sun peppers the heliosphere with impulsive flare material, which starts its journey from compact flare sites narrowly confined to magnetic flux tubes[13], as indicated in Figure 2. Over time and through frequency of occurrence, these particles presumably spread out into another important source distribution. A new comprehensive survey[14] provides clear evidence for the presence of such material in the background population far ahead of the shocks, where acceleration of ^{3}He and heavy ions is observed. This key observation suggests that preexisting energetic and suprathermal particle populations, such as a remnant mixture from impulsive flares and previous CMEs, may be a substantial feeder into particle acceleration, thus indicating an efficient recycling of energetic particles.

A second channel for composition measurements is the distinction of ionic charge states, which are the hallmark of the ionization environment of the source material. Interstellar gas, which streams into the heliosphere as a wind, is a

major player with increasing distance from the Sun (Fig. 2)[15]. These particles appear as pickup ions in the solar-wind plasma and as freshly ionized particles they are mostly singly charged. The, at first, puzzling observation of a substantial He^+ fraction of interplanetary energetic particles[16] in the multiply charged solar wind has found its natural explanation after the detection of interstellar pickup He^+.[17] The identification of pickup ions as the major contributor to energetic He in a CIR at 4.5 AU[18] has led to the suggestion that pickup ions are generally an important source for efficient acceleration at interplanetary shocks[19]. With an average of ≈25%, the He^+ abundance is much reduced at 1 AU compared with its dominance at 4 - 5 AU. But, as shown in Figure 3, the observed increase in He^+/He^{2+} with time elapsed from the start of each CIR reflects the increasing importance of interstellar He as source material with distance from the Sun, as the spacecraft is magnetically connected to the CIR at larger and larger distances[20].

Interstellar pickup ions are also an important contributor at interplanetary travelling shocks. The overwhelming majority of the energetic He^+ at these shocks cannot stem from cold prominence material, even for CMEs that show an overabundance of He^+ in the solar wind bulk flow, as the substantial enhancements in the energetic population occur outside the CME cloud[21,22]. A survey of He^+ and He^{2+} demonstrates that, with $He^+/He^{2+} \approx 0.06$, He^+ is in fact the third most abundant ion species of the energetic-particle population in the inner heliosphere[22].

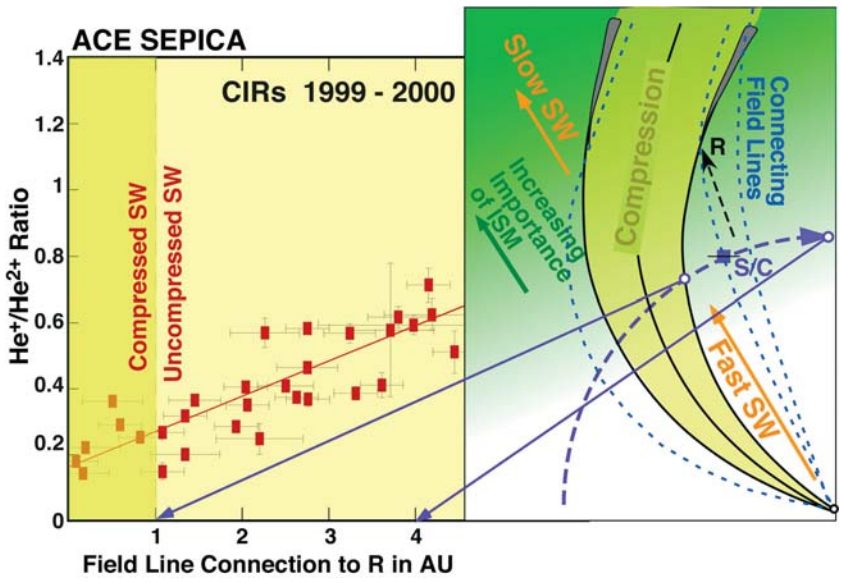

Figure 3. Temporal variation of the He^+/He^{2+} ratio shown as a dependence on the distance of a CIR from the Sun to which the field line at the S/C connects. The rise indicates the increasing importance of interstellar He^+ pickup ions as source.

The relative abundance of He^{+} over He^{2+} is substantially (by 50-200 times) enhanced in the energetic population over the source population, i.e. the abundance ratio of pickup ions over solar wind He^{2+}.

Based on the observed increased injection efficiency of pickup ions into acceleration, it was argued that the "inner source" of pickup ions may also contribute substantially to the energetic particle population in CIRs[19]. The inner source is thought to be solar wind that is implanted in interplanetary dust grains and then re-emitted as neutral atoms[23], or solar wind that is neutralized by penetrating very small dust particles[24], thus leading to a somewhat modified solar-wind composition. Although revealing He^{+} and Ne^{+}, detailed studies of the energetic CIR population at ≈1 MeV/amu did not find any evidence for the expected singly charged C, O, or Mg, and the observed charge state distributions clearly resemble those of the adjacent solar wind[25,26].

Acceleration Processes

In a nutshell, particle distributions that feature a high-energy extension from the bulk flow, such as remnant energetic particles and pickup ions, appear to be efficiently accelerated further. To discuss the acceleration processes, it is therefore justified to start with particles that already have a wide velocity distribution compared with the relatively cold bulk plasma. We will leave the question of how particles make the transition into this suprathermal distribution until the last chapter. Under this premise, the particles are rather mobile in the frame of the bulk plasma. Their motion can be altered by obstacles in the bulk flow, which we term "scattering centres", and they have the ability to cross discontinuities between plasmas of different velocity freely. It is these qualities that make the particles susceptible to acceleration.

First-order Fermi acceleration

First-order Fermi acceleration is an unavoidable consequence in the presence of any jump in plasma bulk velocity V_b, if particles cross such a jump multiple times and undergo multiple collisions[27]. A pictorial view of this process is shown in Figure 4 for a parallel shock, i.e. the magnetic field is parallel to the shock normal. Plasma with embedded magnetic field and fluctuations is approaching from the left with high speed (indicated by the blue arrows). It then slows down either abruptly at a shock (upper half) or gradually in a compression region (lower half). The transition in speed V_b is indicated in the two graphs above and below the main figure and by the shorter red arrows. Grey shading indicates the related compression in density. Particles that move already relative to the bulk flow may get turned around by magnetic fluctuations (indicated as scattering

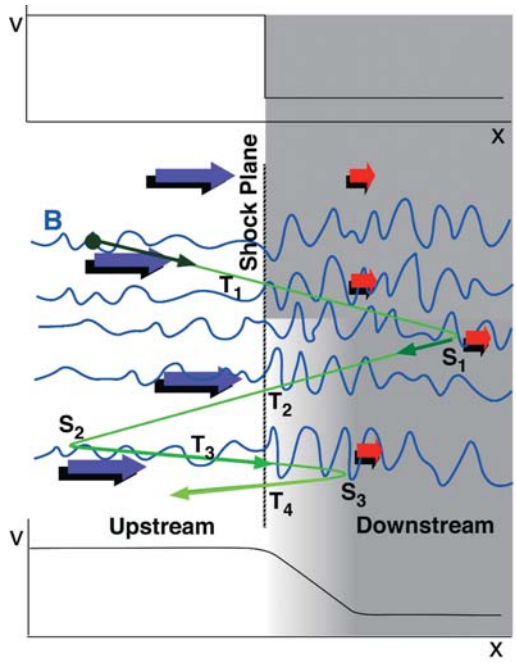

Figure 4. Schematic representation of first-order Fermi acceleration for plasma flow with embedded magnetic-field fluctuations. Ions with motion relative to the flow gain energy through a combination of scattering ($\mathbf{S_i}$) upstream and downstream and transitions ($\mathbf{T_i}$) of the speed change, independent of the smoothness of the change. Speed is shown as line plots and the related density change as grey shading. Top: Strong shock; Bottom: Gradual change.

events $\mathbf{S_i}$), which may be described like an elastic collision with a massive partner, as the magnetic field is strongly coupled to the bulk flow. After one complete cycle of scattering downstream ($\mathbf{S_1}$) and upstream ($\mathbf{S_2}$) with dual transition ($\mathbf{T_1}$, $\mathbf{T_2}$) of the velocity gradient, the original momentum mv_i has increased to $mv_f = mv_i + 2m(V_u - V_d)$, where V_u and V_d are the upstream and downstream values of the flow speed. Consecutive cycles add momentum in equal increments.

Figure 5 shows the process in velocity space in terms of the classical Fermi acceleration "picture"[28]. The velocity space trajectories, shown here in the reference frame of the shock, describe the velocity evolution for the sample ion in Figure 4. It starts out somewhat faster than the solar wind and thus is already suprathermal. Scattering at magnetic field fluctuations occurs approximately under conservation of energy in the plasma frame, for $\mathbf{S_1}$ the slow or shocked flow (red dot). The square of the total ion speed $v^2 = v_{||}^2 + v_{\perp}^2$ is conserved in the downstream flow, where $v_{||}$ and $v_{\perp}$ are the velocity components parallel and perpendicular to the magnetic field. As a consequence, the trajectory is a circular arc centred on the downstream flow velocity. Once the ion's parallel velocity is negative in the shock frame, it can cross the shock and reach the upstream plasma ($\mathbf{T_2}$). Here the ion is scattered on a sphere around the blue dot ($\mathbf{S_2}$) so that it reaches a positive speed in the shock frame and comes back to the downstream plasma ($\mathbf{T_3}$). Apparently, the ion gains energy with each shock crossing, as evidenced by the increasing radii of the arcs.

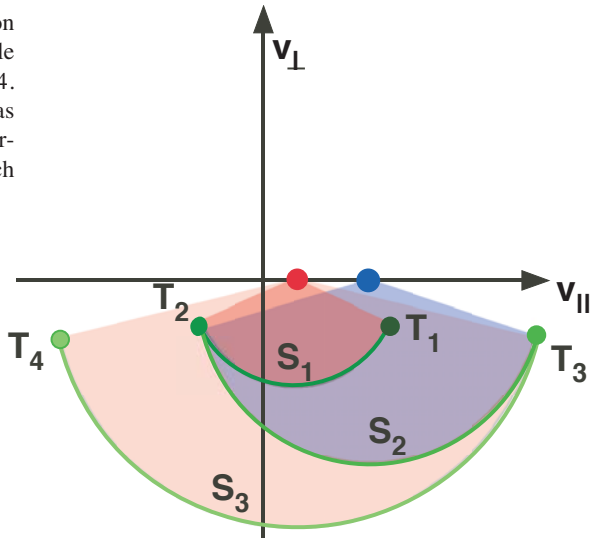

Figure 5. Schematic view of the ion velocity evolution for the sample trajectory shown in Figure 4. Increases in energy show up as increases in the radii of the scattering arcs in velocity space after each transition of the discontinuity.

As seen in Figure 4, also a smooth transition with the same overall speed change can produce the same increment of acceleration, if the ion is scattered after passing the full gradient[29]. The average momentum or energy gain in a smooth transition is less efficient though, because not all particles traverse the full speed change. The ratio of the mean free scattering length and the scale length of the gradient determines the overall acceleration efficiency. This extension of shock acceleration appears to be a natural explanation for the, at first, puzzling observation that CIRs can also accelerate particles at 1 AU, without fully developed shocks[30].

Second-order Fermi acceleration

In the presence of magnetic-field fluctuations, which provide the means of cross-shock transport, ions are also scattered back and forth between plasma waves with different velocities in the plasma frame. This leads to second-order Fermi acceleration (or acceleration of ions in turbulent plasma waves), which is also a natural consequence of particle transport[31]. If we consider for a moment two waves that propagate in the same direction, but at fast and slow speeds, respectively, we can associate these speeds with the blue and red dots in Figure 5 and treat particle acceleration accordingly. However, waves may propagate in random directions, even in opposite directions. Depending on whether a particle is scattered at a wave in a head-on or an overtaking collision determines the energy change. Particles gain momentum (and energy) in head-on scattering, but lose it in overtaking scattering, making second-order Fermi acceleration a stochastic process. However, the scattering rate is also proportional to the relative velocity of particle and scatterer. Thus head-on scattering is more frequent, leading to a net momentum and energy gain.

Compared with first-order Fermi acceleration, whose strength derives from the change in the bulk velocity (V_b) at a discontinuity, second-order Fermi acceleration depends on the random speed of scattering centres in the plasma, or the speed of the prevalent waves (Alfvén or sound speed). Therefore, first-order Fermi acceleration is usually stronger than its second-order cousin in supersonic or Alfvénic flows with discontinuities by a factor of M^2 in terms of energy gain, where M is the Mach number. However, in the absence of discontinuities second-order Fermi acceleration may become the dominant process. Relating to the pictorial view in Figure 5, the second-order process also relies on momentum change during scattering, but now in the wave frame. The increment in momentum change is determined by the wave speed relative to the plasma. Effective scattering and randomization of momentum, and thus acceleration, is achieved if more than one wave mode and/or propagation direction is present.

Acceleration efficiency and escape

Let us now ask how efficient acceleration can be, and do this while concentrating on first-order Fermi acceleration, as the arguments follow in a similar way for the second-order process. Fermi acceleration requires elastic scattering of an ion in both the upstream and downstream plasmas. This is the only way in which the plasma can "communicate" the speed difference between upstream and downstream to the ion to energize it during each round trip across the shock. There are two limits beyond which first-order Fermi acceleration may not work. Firstly, the ions are scattered too strongly in the downstream plasma, will simply be convected away, and will never return to the upstream plasma. Secondly, the ions are scattered too weakly either in the upstream or in downstream plasma. In that case they will not be energized through "ping-pong collisions" with the plasmas of different speeds in reasonable time.

To be efficiently accelerated, particles have to cross the shock or discontinuity multiple times. For a parallel shock the ions are rather mobile, as they cross in the direction of the magnetic field lines. Therefore, they finish many round trips during the lifetime of the shock. An interplanetary shock can accelerate ions that are observed near Earth during the time it travels from the Sun to Earth, typically a few days. An estimate of the average time for an ion to revert to its "parallel" speed along the mean interplanetary magnetic field is roughly 1 to 10 minutes. This is sufficiently short for the ions to undergo efficient acceleration, in agreement with observations.

If first-order Fermi acceleration were to continue unabated at a planar shock, a power law spectrum in energy E for the differential flux $j(E) = j_o \cdot (E/E_o)^{-\gamma}$ results[32], whose spectral index γ is related to the shock compression ratio r as $\gamma = (r+2)/2(r-1)$. In any realistic situation though, the energy spectra are estab-

lished in a balance between acceleration and escape from the finite acceleration region. As diffusive transport of particles usually speeds up as a function of the magnetic rigidity R, which scales in the non-relativistic limit as $R \sim v \cdot A/Q$, with atomic mass A and ionic charge Q, the spectra turn over into an exponential behaviour at high energies. This turnover occurs at lower energies for particles with higher A/Q values, as observed for heavier species[33].

Quasi-perpendicular shocks and drift acceleration

So far our models apply to a quasi-parallel shock (or compression). However, often the field is oriented oblique or even nearly perpendicular to the shock normal, which is typical for CIRs beyond 1 AU. This is a quasi-perpendicular shock, which allows also for another acceleration process, i.e. shock drift acceleration.

This process is based on the convective electric field in magnetized plasma, moving with velocity $\boldsymbol{V}_b$ perpendicular to the magnetic field $\boldsymbol{B}_0$. Protons take a right turn around the magnetic field $\boldsymbol{B}_0$ and electrons a left turn due to the Lorentz force. The charges separate, and an electric field $\boldsymbol{E}$ builds up ($E = V_b B_0$), which is perpendicular to $\boldsymbol{V}_b$ and $\boldsymbol{B}_0$. Ions with velocity $\boldsymbol{V}_b$ do not feel this field at all. With a different velocity, they feel it on their gyro-orbits alternately against and with their motion. In both cases there is no net effect on the ion energy. The situation changes at a shock. An ion that gyrates half of its orbit upstream and half downstream experiences two different field strengths, usually larger upstream. This leads to a net acceleration without scattering, while the ion drifts along the shock surface for a short distance. After this encounter, the ion usually is swept downstream with the flow, and it needs scattering to allow multiple shock encounters for further energy gain.

Multiple scattering and thus Fermi acceleration of both kinds work best when the ions can move freely between upstream and downstream, or between randomly moving scattering centres, without the need to cross magnetic field lines. At a perpendicular shock all ions are effectively swept into the shock (or compression) due to their gyro-motion, but return into the upstream region is severely hampered. In order to move back upstream the ions must now be scattered across field lines. Only a rather small fraction of the ions, which scales with the fraction $\eta = \delta B^2/B_0^2$ of magnetic energy present as fluctuations, will cross the shock again after each cycle. In a simplified way, we can express the capability to return upstream in terms of a diffusion speed across field lines $v_D = \eta v$, where v is the actual ion speed. For typically small η values, the ions need a high speed. Of course, ions may also cross oblique shocks along field lines, but the escape speed required is increased over the downstream flow speed by $1/\cos\Theta$, where Θ is the angle between the magnetic field and the shock normal. For nearly per-

pendicular shocks, this speed is enormous. As one can imagine, a high enough speed is hardest to attain at the very beginning of the acceleration.

Injection Problem

After exploring the efficiency and limits of acceleration and learning that often shock acceleration is most effective, we need to turn our attention to the start of the process. In fact there is an obstacle to shock acceleration, the injection problem, and thus far it is not solved. In the ISSI book on CIRs, the injection problem is spelled out as the major unsolved problem of shock acceleration[5]. All possible injection mechanisms are summarized, with special emphasis on perpendicular shocks, as is relevant for CIRs, but no convincing model that overcomes all problems is presented[31]. This situation has not changed since.

It is not only the scattering rate that decides on the success of the first-order Fermi process, but also the ion speed. Ion speed and scattering rate combine into the mean free path, which directly relates to ion mobility. If the mobility of an ion in the downstream plasma is sufficiently high, it has some chance of being returned to the upstream plasma against the downstream plasma flow. The mean free path usually increases with ion speed. However, this is not the only necessary condition for shock acceleration to start. Upon approaching the shock from downstream after their first scattering or from the tail of the heated distribution, the ions need a minimum speed to outrun the shock. This minimum speed with which an ion has a reasonable chance of being returned to the upstream plasma is called the *injection threshold*. It is very different for the two types of shocks, parallel and perpendicular, as it depends strongly on the angle Θ between magnetic field and shock normal.

Injection at quasi-parallel shocks

We start with the type of shock where ions have little problem to undergo a first-order Fermi acceleration. At quasi-parallel shocks, the magnetic field is almost parallel to the shock normal, i.e. perpendicular to the surface of the shock front. To initiate the multiple shock crossing an ion needs to be able to return upstream, or its minimum escape speed from the downstream region must exceed the downstream flow speed.

The sample ion depicted in Figure 4 does not seem to have difficulties to return upstream after the first scattering in the downstream region, as it is deliberately chosen as a suprathermal ion. Even when solar wind ions reach the downstream region without changing velocity at the shock, they would constitute a suprathermal population to which the above-mentioned scattering theory applies.

However, this picture is incomplete because it omits the shock potential, which slows down the vast majority of the solar wind ions (blue dot in Fig. 5) to the downstream bulk distribution (red dot). No scattering would ensue in the downstream region, and the injection problem persists for solar-wind ions that are close to the bulk distribution.

To discuss the injection for different particle populations, Figure 6 shows a compilation of various distributions in interplanetary space in a two-dimensional projection and as a one-dimensional cut. All ions that are close to the solar-wind bulk velocity, i.e. almost all of the genuine solar-wind ions (yellow) will mostly be decelerated so that they do not experience any scattering. However, there are several much more extended distributions, for which the described injection scenario works particularly well. The first are interstellar pickup ions (dark blue), whose velocity distribution is approximately described by a sphere in velocity space, centred on the solar wind, with a radius equal to the solar-wind speed. Therefore, these ions are already "suprathermal," and they have the "pole position" for acceleration. Ions that have already experienced prior acceleration, as indicated by the light blue distribution in Figure 6, have a similar advantage. This explains why both interstellar pickup ions and remnant energetic ions are found with substantially increased abundance over solar-wind ions in CIRs and at travelling shocks. Inner source pickup ions could also be viewed as suprathermal, as they are separate from the solar-wind bulk. However, they are generally slower than the solar wind. Since they do not appear efficiently accelerated at least at 1 AU, perhaps mostly particles that are already faster than the solar wind are preferentially injected.

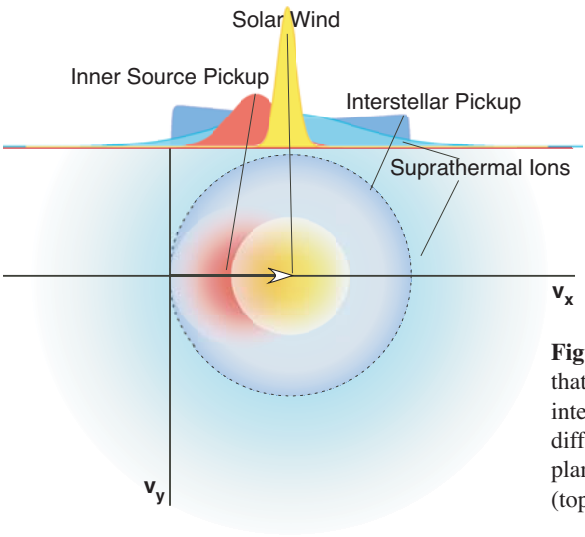

Figure 6. Velocity distributions of ions that can be injected into acceleration in interplanetary space are indicated with different colour shading in the $v_x - v_y$ plane (bottom) and as a cut in the v_x axis (top).

Injection at quasi-perpendicular shocks

Injection at a perpendicular shock is much more problematic. Let us follow the simplified view that first-order Fermi acceleration at a perpendicular shock operates for a diffusion speed ηv, which is larger than the downstream bulk speed V_d in the shock frame. For typical values of $\eta \approx 0.01$, the ion speed must be of order 5000 km/s, even if the downstream bulk speed is rather low, i.e. 50 km/s. 5000 km/s (equivalent to energies of >125 keV/amu) obviously is much higher than a typical solar-wind speed of 400 –700 km/s, and it is not clear yet how ions reach the injection speed, exemplifying the "injection problem."

The standard model of the perpendicular mean free path may be oversimplified[34], as magnetic field line "braiding" could increase the scattering efficiency by a factor 2 to 5. This would reduce the injection threshold to ≈ 25 – 60 keV/amu at CIRs, and numerical simulations revealed that at least a fraction of the interstellar pickup ions are fed into the first-order Fermi process at a perpendicular shock, but almost none of the thermal solar-wind ions. This is consistent with the observations that pickup ions are preferentially injected into acceleration at CIRs[19]. However, energetic particles with solar-wind composition are also observed at CIRs, and the assumption of increased perpendicular mean free paths has not yet been verified experimentally.

One interesting process is that of shock surfing[35,31], a special form of shock drift acceleration. In Figure 7 a pickup ion reaches the shock with very low speed, is reflected by the electric cross-shock potential, and then experiences the upstream convective electric field during a fraction of its gyro-period until it is reflected again[36]. Ultimately, such an ion reaches a speed that enables it to cross the shock, which often exceeds the injection threshold. However, the process is very idealized and only works for a shock that is perpendicular and planar over a large spatial scale and whose width is smaller than the ion gyro-radius. For typical shock widths observed in interplanetary space, the ions may reach a few 10 keV/amu, barely enough to reach the injection threshold. Again, this process works much better for pickup ions than for solar-wind ions because pickup ions populate velocity space below the bulk speed and a fraction always coincides with the shock velocity.

Alternatively, pre-acceleration by second-order Fermi acceleration has been suggested[31], which again prefers suprathermal, or typically super-Alfvénic, ion populations. Super-Alfvénic means that - in the bulk plasma frame - ions are faster than the Alfvén speed (the speed with which magnetic disturbances propagate in the solar-wind plasma regardless of frequency, $V_A \approx 50$ km/s). This also discriminates strongly against thermal solar wind and still leaves us with the question of

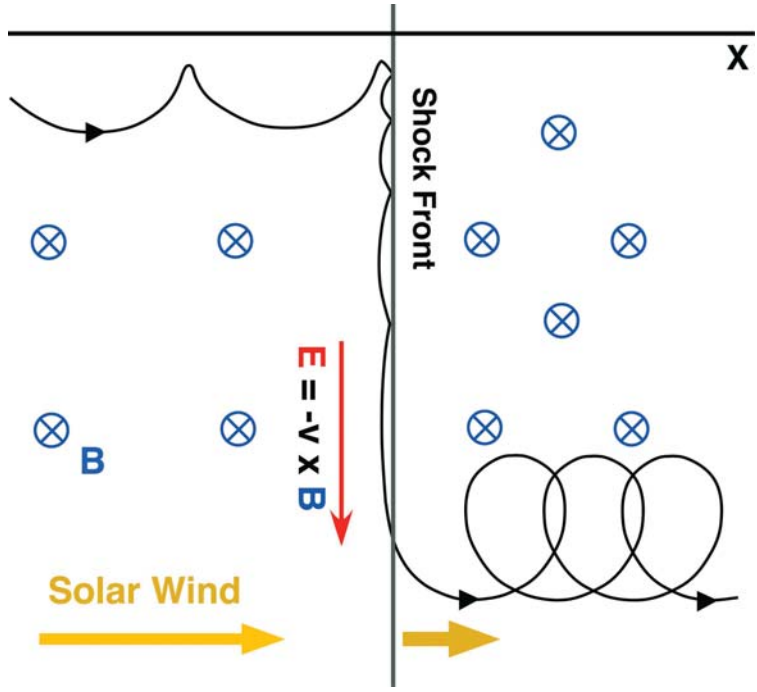

Figure 7. Schematic view of a shock surfing trajectory. An ion that arrives at the shock front with low speed in the shock frame from the left gains energy in the convective electric field in the course of several bounces.

how solar wind ions of only 1 keV/amu are pre-accelerated for injection at CIRs. Even the injection of pickup ions currently cannot be described quantitatively.

Particle Acceleration: The Bigger Picture

In summary, we have achieved a solid understanding of the basic processes that contribute to particle acceleration in the heliosphere. With a big step in the sensitivity and collection power of particle instrumentation that allows us to clearly distinguish elements, isotopes, and ionic charge states from solar-wind energies to those of cosmic rays, we have identified several different key sources that feed substantially into the energetic particle populations, such as solar wind, corona, interstellar pickup ions, possibly pickup ions from other heliospheric sources, impulsive flare plasma, and re-cycled energetic particle populations themselves. We are able to sample in detail energetic particle populations in the making at the Earth's bow shock, at interplanetary travelling shocks in CMEs, and at the shocks related to CIRs. We have sampled at least briefly the other planetary shock waves, and possibly we will have clear *in-situ* evidence from acceleration at the termination shock in the near future.

The ISSI book on CIRs paints a clear picture of the acceleration of two distinct and relatively clean sources during solar-minimum conditions, solar-wind and interstellar pickup ions, mostly unpolluted by solar energetic-particle events. This effort has led to the relatively broad consensus that Fermi acceleration is at work, most prominently at the reverse shock, and that even when no shock has yet formed a similar process is effective in the compression region, just not as strong yet. The book also contains compelling evidence from various observations that interstellar pickup ions have a clear advantage to be accelerated. The follow-on conjecture that dust related inner source ions should also have a similar advantage has led to a search that has given us a negative answer so far for observations at 1 AU. Together these pieces of evidence provide us with clues and constraints on the still vexing injection problem. The ISSI book on CIRs has compiled the current ideas on how solar-wind or pickup ions take the first step towards acceleration, but no convincing conclusions are yet on the horizon, even five years after the CIR effort. The infusion of ideas towards a resolution may come from the microscopic and multi-point study of the bow shock that is underway with Cluster, aided by extensive simulations. A workshop at ISSI has taken a current snapshot, which is also being discussed among other aspects in this volume. A compilation of the acceleration scenarios in CMEs during the solar-maximum phase with an even more complex source composition is underway in the ISSI book on CMEs[6].

The quantitative description of the acceleration regions in the inner Solar System, for which we have a plethora of *in-situ* observations, as touched upon in this article, will be the stepping stone towards understanding the largest shock in our home system, the solar-wind termination shock. By applying appropriate scaling laws, we can also transfer this knowledge to particle acceleration on the grand scale in astrophysics, i.e. to supernova shock waves and galactic winds, where we are convinced the birthplace of the much more energetic galactic cosmic rays lies. In the end, we will have to solve the remaining puzzles, such as the injection problem, through detailed studies on our own doorstep, before we can apply the new insight to regions that we can only access with remote sensing. To combine the ever-increasing body of information into a comprehensive view and to build interdisciplinary bridges between *in-situ* analysis and remote-sensing observations, ISSI provide a unique forum, which has already created and continues to create links that were not there before[37].

References

1. R. Diehl, E. Parizot, R. Kallenbach & R. von Steiger (Eds.), "The Astrophysics of Galactic Cosmic Rays", Space Sci. Ser. of ISSI Vol. 13, Kluwer Acad. Publ., Dordrecht, and *Space Sci. Rev.*, **99**, Nos. 1-2, 2002.
2. J.W. Bieber, E. Eroshenko, P. Evenson, E.O. Flückiger & R. Kallenbach (Eds.), "Cosmic Rays and Earth", Space Sci. Ser. of ISSI Vol. 10, Kluwer Acad. Publ., Dordrecht, and *Space Sci. Rev.*, **93**, Nos. 1-2, 2000.
3. L.A. Fisk, J.R. Jopikii, G.M. Simnett, R. von Steiger & K.-P. Wenzel (Eds.), "Cosmic Rays in the Heliosphere", Space Sci. Ser. of ISSI Vol. 3, Kluwer Acad. Publ., Dordrecht, and *Space Sci. Rev.,* **83**, Nos. 1-2, 1998.
4. R.A. Mewaldt, R.C. Ogliore, G. Gloeckler & G.M. Mason, in: *Solar and Galactic Composition*, R. Wimmer (Ed.), *AIP Conf. Proc.,* **598**, 393, 2001
5. A. Balogh, J.T. Gosling, J.R. Jokipii, R. Kallenbach & H. Kunow (Eds.), "Corotating Interaction Regions", Space Sci. Ser. of ISSI Vol. 7, Kluwer Acad. Publ., Dordrecht, and *Space Sci. Rev.*, **89**, Nos. 1-2, 1999.
6. H. Kunow, N. Crooker, J. Linker, R. Schwenn & R. von Steiger (Eds.), "Coronal Mass Ejections", Space Sci. Ser. of ISSI, Kluwer Acad. Publ., Dordrecht, and *Space Sci. Rev.* in prep., 2004.
7. F.B. McDonald, B.J. Teegarden, J.H. Trainor, T.T. von Rosenvinge & W.R. Webber, *Astrophys. J.,* **203**, L149, 1976.
8. G.M. Mason & T.R. Sanderson, in Ref. 5, p. 77.
9. D.V. Reames, *Space Sci. Rev.,* **90**, 413, 1999.
10. G.M. Mason, J.E. Mazur & J.R. Dwyer, *Astrophys. J.*, **525**, L133, 1999.
11. R. von Steiger *et al.*, *J. Geophys. Res.,* **105**, 27217, 2000.
12. D.V. Reames, *Astrophys J. Suppl.* **73***,* 235, 1990.
13. J.E. Mazur *et al., AIP Conf. Proc.,* **528**, 47, 2000.
14. M.I. Desai *et al., Astrophys. J.*, **588**, 1149, 2003.
15. R. von Steiger, R. Lallement & M.A. Lee (Eds.), "The Heliosphere in the Local Interstellar Medium", Space Sci. Ser. of ISSI Vol. 1, Kluwer Acad. Publ., Dordrecht, and *Space Sci. Rev.,* **78**, Nos. 1-2, 1996.
16. D. Hovestadt, G. Gloeckler, B. Klecker & M. Scholer, *Astrophys. J.,* **281**, 463, 1984.
17. E. Möbius *et al.*, *Nature,* **318**, 426, 1985.
18. G. Gloeckler *et al.*, *J. Geophys. Res.,* **99**, 17637, 1994.
19. G. Gloeckler, in Ref. 5, pp. 91-104.
20. D. Morris *et al.*, *AIP Conf. Proc.,* **598**, 201, 2001.
21. K. Bamert *et al.*, *J. Geophys. Res.,* **107**, 1130, 2002.
22. H. Kucharek *et al.*, *J. Geophys. Res.,* **108**, 8030, doi: 10.1029/2003JA009938, 2003.
23. J. Geiss, G. Gloeckler & R. von Steiger, in Ref. 15, pp. 43-52.
24. R.F. Wimmer-Schweingruber & P. Bochsler, *Geophys. Res. Lett.,* **30**, 1077, doi: 10.1029/2002GL015218, 2003.

25. E. Möbius *et al., Geophys. Res. Lett.,* **29**, 1016, 2002.
26. J.E. Mazur, G.M. Mason & R.A. Mewaldt, *Astrophys. J.,* **566**, 555, 2002.
27. M. Scholer in Ref. 5, pp. 105-114.
28. T. Sugiyama & T. Terasawa, *Adv. Space Res.*, **24**, 73, 1999.
29. J. Giacalone, J.R. Jokipii & J. Kota, *Astrophys. J.*, **573**, 845, 2002.
30. G.M. Mason *et al.*, in Ref. 5, pp 327-367.
31. M. Scholer *et al.*, in Ref. 5, pp. 369-399.
32. F.C. Jones & D.C. Ellison, *Space Sci. Rev.,* **58**, 259, 1991.
33. D.C. Ellison & R.R. Ramaty, *Astrophys. J.,* **298**, 400, 1985.
34. L.A. Fisk & J.R. Jokipii, in Ref. 5, pp. 115-124.
35. R.Z. Sagdeev, *Rev. of Plasma Phys.,* **4**, 23, 1966.
36. M.A. Lee, V.D. Shapiro & R. Sagdeev, *J.Geophys. Res.*, **101**, 4777, 1996.
37. E.M. would like to thank the International Space Science Institute and the Physikalische Institut at the Universität Bern for their hospitality during the preparation of this paper and gratefully acknowledges the support by the Hans-Sigrist Stiftung. The work was supported under NASA Grants NAG5-10890 and 12929 and INTAS Grant WP 01-270.